Solid State NMR Characterization and Adsorption Properties of Lignocellulose-Clinoptilolite Composites Prepared with Siloxanes Coupling Agents

R.M.K. Vala[a,c,*], L. Tichagwa[a], H. Pasch[b] and E.D. Dikio[c]

[a]*Formerly, Department of Pure and Applied Chemistry, University of Fort Hare, Private Bag X1314, Alice, 5700, South Africa.*

[b]*Deparment of Chemistry and Polymer Science, University of Stellenbosch, Private Bag X1, Matieland, 7602, Stellenbosch, South Africa.*

[c]*Deparment of Chemistry, Applied Chemistry and Nanoscience Laboratory, Vaal University of Technology,
P.O. Box X021, Vanderbijlpark, 1900, South Africa.*

ABSTRACT

This study reports the preparation of lignocellulose-clinoptilolite composites by means of N-terminated siloxanes as coupling agents, after acid hydrolysis. Reactions were carried out in the presence of dibutyltin dilaurate as catalyst by reacting lignocellulose modified with the coupling agents and clinoptilolite at 140 °C in DMF under nitrogen atmosphere. The light in weight and fluffy composites obtained were characterized by FT-IR, XRD, TGA, SEM and Solid State NMR. Results depicted possible chemical interactions between the two materials (lignocellulose and clinoptilolite). Used as adsorbents, the composites showed to be good candidates for the removal of used motor oil from aqueous solution, with up to 92 mg g^{-1} of chemical oxygen demand removed.

1. Introduction

Over the last few years, researchers have been investigating the use of natural fibres as constituents of composite materials. Such investigation has increased because of the relative low cost, ability to be recycled, and the fact that these materials can compete well in terms of strength per weight.[1–4] Also, the composites are environmentally friendly, fully degradable and sustainable, and at the end of their life spans, can be easily disposed or composted without harming the environment.[2,3]

Developed to produce materials with performance that combines the positive attributes of each component for various applications, the preparation of composites is challenged at the interface between the filler and the matrix,[5] causing problems, such as poor compatibility, insufficient stress transfer, and high water uptake. Organic–inorganic composites have interesting mechanical, optical, electrical and thermal properties compared to those of the starting materials;[6] however, the differences in the individual intermolecular interaction forces, the interfacial incompatibility between the materials often cause failures in the preparation of composites to achieve homogeneous mixture.[7,8] Moreover, if natural fibres are used as matrix, an improvement in filler–matrix adhesion is usually achieved by filler surface or matrix (fibres) modifications, addition of compatibilizers or coupling agents.[8] Therefore, compatibility of components of composites is one of the major challenges encountered which necessitate the use of a bridge to bring materials together.

Lignocellulose is used in composites for being abundant, non-hazardous and of relative low cost in addition to it being eco-friendly, biodegradable, renewable, of low density. It has gained widespread use in the plastics, automobile, packaging industries,[9–11] and many point it out as adsorbent and thermoplastics material.[12–15] Although some authors reported the preparation and use

of lignocellulose-zeolite composites, most of them have used cellulose, instead of the lignocellulose complex. Fisher.[16] used polyethylene, polypropylene and poly(vinylchloride) as coupling agents to prepare wood-zeolite composites. Most of zeolites composites have been prepared either with synthetic polymers such as organosiloxanes[17] or activated carbon-derived lignocellulose.[18] As for lignocellulose-clinoptilolite composites, very little was found in the literature probably because of two reasons: (1) the weak interaction between the two materials and the uneven distribution of zeolite on the lignocellulose surface as reported by Mintova and Valtchev[19] and (2) their individual efficiency in different applications. It therefore seemed essential to investigate the preparation of lignocellulose-clinoptilolite composites and evaluate their sorptive properties towards water pollutants, such as motor oil.

Used motor oil is a harmful polluting product; its disposal should be done with environmental concerns. It was shown that biodegradation of motor oil can last for years depending on factors, such as: low numbers of microbes, insufficient oxygen or nutrient availability, temperature and water availability.[20–22] Researchers[23,24] have pointed out the adverse effects of used motor oil on the environment, regarding oil as capable of generating carcinogens and endocrine disrupters[25–27] and interfering with respiration across gill surfaces of fishes and other animals.[28] Unfortunately, routine maintenance of vehicles ends up polluting water bodies with oil, especially in developing countries. Thus, sorbent materials (cotton, milkweed, kenaf vegetable, wool fibres and clay mineral) have been tested for the removal of oil from water,[29–35] giving promising results.

However, to the best of the authors' knowledge, there is no report in the literature on the preparation, solid state NMR characterization of lignocellulose-clinoptilolite composites prepared with N-terminated siloxanes as coupling agents, and their use as adsorbents, especially for the removal of used motor

* To whom correspondence should be addressed. E-mail: mavularemy@gmail.com

oil. Therefore, this study presents the preparation of ligno-cellulose-clinoptilolite composites with siloxanes (coupling agent) and dibutyltindilaurate (catalyst). The composites (characterized by FT-IR, XRD, SEM, TGA and solid state NMR) were used as adsorbent for the removal of motor oil from aqueous solution.

2. Experimental

2.1. Materials

Siloxanes (3-aminopropyl-terminated polydimethylsiloxane, molecular weights: 1000, 2600, and 11000 g mol^{-1} for siloxane NH15D, NH40D, and NH130D, respectively) used as coupling agents were supplied by Wacker Chemie AG, Germany, dibutyl-tindilaurate (DBTDL) and dimethylformamide (DMF) by Sigma Aldrich; all were used without further modification. Kikuyu grass (*Pennisetum clandestinum*) was collected from gardens at the University of Fort Hare (Eastern Cape, South Africa), and used as source of lignocellulose. Clinoptilolite was obtained from Cape Bentonite (Pty) Ltd. (Heidelberg, Western Cape, South Africa). Used motor oil (collected from a garage in Alice, Eastern Cape, South Africa) was filtered (Whatman filter paper, 150 mm ø) and oven-dried in an open vessel for 48 h at 60 °C with frequent shaking. The properties of the oil are summarized (Table 1).

Table 1 Properties of used motor oil.

Parameter	Value
Water content (w/w %)	6.9
Density (kg m^{-3})	882
Viscosity (mPa·s) (by DV-E Viscometer at 50 rpm)	420
Inorganic content (w/w %)	0.5

2.2. Clinoptilolite Treatment

Clinoptilolite was pre-treated according to the literature[36–39] as follows: 20 g of raw clinoptilolite were ground into powder in order to pass through a 425 μm U.S sieve. The powder obtained was refluxed in HCl (0.25N) for 6 h at 96 °C in order to extract impurities. After filtration, the residue was thoroughly washed, first with cold and then with hot deionized water, until all traces of acid were removed and the AgNO$_3$ chloride test proved negative. The purified clinoptilolite was then calcinated at 300 °C for 8 h.

2.3. Grass/Lignocellulosic Material Treatment

Grass was pre-treated according to the procedure obtained from Ruiz and Ehrman[40] and Palmowski and Muller.[41] Soluble substances were extracted by decoction for 30 min. The mixture was filtered and the residue thoroughly water washed until the filtrate became 'colourless'. The solid residue (lignocellulose) was oven-dried overnight at 65 °C and then fractionated (hydrolyzed) in H$_2$SO$_4$ according to the literature[42–45], prior to chemical modification.

The chemical modification of lignocellulose by siloxanes was adapted from the work of Matías[46] and Le Digabel[47] and carried out as follows: in a 3-neck round-bottomed flask, 10 mL of 3-aminopropyl-terminated polydimethylsiloxane were added to 1.5 g of lignocellulose in 30 mL of DMF and refluxed for 5 h at 130 °C. The reaction was carried out under N$_2$, in the presence of 200 μL of DBTDL. The product was Soxhlet extracted with 100 mL THF for 5 h. The resulting materials were oven-dried overnight at 65 °C and designated as: LNH15D (lignocellulose modified with siloxane NH15D), LNH40D (lignocellulose

modified with siloxane NH40D) and LNH130D (lignocellulose modified with siloxane NH130D).

2.4. Preparation of Lignocellulose-Clinoptilolite Composites

Lignocellulose-clinoptilolite composites were prepared by reacting the chemically modified lignocellulose with clinoptilolite. The composites were prepared according to a procedure adapted from Cao[48] as follows: required amounts of lignocellulose modified with siloxanes were added to 50 mL of DMF, then required amounts of clinoptilolite powder were slowly added to the mixture and stirred at room temperature for 30 min. Temperature was then raised up to 140 °C and stirred under N$_2$ for 5 h to yield the composites. Unreacted chemicals were Soxhlet extracted from composites with 50 mL of THF for 5 h and overnight dried at 65 °C. The mass ratio of lignocellulose modified with siloxane to clinoptilolite was 2:1. The composites were then thoroughly washed with deionized water and overnight dried at 65 °C. The resulting composites were designated as: CNH15D (composite prepared with siloxane NH15D), CNH40D (composite prepared with siloxane NH40D) and CNH130D (composite prepared with siloxane NH130D). The fibrous materials obtained were fawn in colour, spongy and fluffy.

2.5. FT-IR, XRD, TGA and SEM Characterization

All the materials were characterized by FTIR in a matrix of KBr by means of a Perkin Elmer System 2000 FTIR spectrophotometer (Perkin Elmer, Beaconsfield Bucks, England). X-ray diffraction (XRD) patterns were obtained using a Bruker D8 Advance diffractometer (Bruker, Germany) with CuKα radiation (λKα_1 = 1.5406 Å) at 40 kV and 40 mA. The thermogravimetric analysis (TGA) was evaluated on TGA-7 Perkin Elmer Pyris (heating rate of 20 °C min^{-1} at the temperature range of 20–900 °C in static atmosphere, weight of samples taken in the range of 7.6–9.8 mg). The surface morphology was examined by scanning electron microscopy (SEM) with a JEOL JSM-6390 LV scanning electron microscope (from JOEL, Tokyo, Japan), using an accelerating voltage of 15 kV.

2.6. Experimental for ^{13}C Solid State NMR Analysis

The solid state (SS) NMR spectra were acquired on a Varian (VNMRS WB 500 solids) static magnetic field strength: 11.7 T (corresponding to a proton larmor frequency of 500 MHz) two-channel spectrometer using 6 mm zirconia rotors and a 6 mm Chemagnetics™ T3 HX MAS probe. The ^{13}C{^{1}H} cross-polarization (CP) spectrum was recorded at ambient temperature with high-power proton decoupling using a recycle delay of 5 s on the composite sample as well as the lignocellulose. The power parameters were optimized for the Hartmann-Hahn match; the radio frequency fields were Y$_C$B$_{1C}$ = Y$_H$B$_{1H}$ ≈ 56 kHz. The contact time for cross-polarization was 1 ms. Magic angle spinning (MAS) was performed at 5 kHz and adamantane was used as an external chemical shift standard where the downfield peak was referenced to 38.3 ppm. Additionally ^{13}C{^{1}H} CP MAS experiments with total spinning sideband suppression (TOSS) were performed.

2.7. Experimental ^{29}Si SS NMR Analysis

The clinoptilolite and composite samples were studied using ^{29}Si SS NMR on a Varian spectrometer (VNMRS WB 500 solids) static magnetic field strength: 11.7 T (corresponding to a proton lamor frequency of 500 MHz) two-channel spectrometer using 6 mm zirconia rotors and a 6 mm Chemagnetics⁻ T3 HX MAS probe. One-pulse MAS experiments were performed at a spinning frequency of 5 kHz using a pulse length of 5 μs. The spectra

were measured under partially relaxed conditions. The power parameters of the ^{29}Si{1H} CP MAS experiments were optimized for the Hartmann-Hahn match; the radio frequency fields were $\gamma_C B_{1C} = \gamma_H B_{1H} \approx 56$ kHz. The contact time for cross-polarization was 2 ms and the recycle delay used was 3s. The ^{29}Si one-pulse MAS spectra of clinop-HCl measured with and without spinning sideband suppression was conducted.

2.8. Experimental Procedure for the Adsorption of Motor Oil

Adsorption experiments were conducted with used motor oil (adsorbate) that was emulsified in deionized water and then used as oily wastewater as follows: a known amount (200, 400, 600, 800, 1000 mg) of oil was ultrasonicated for 20 min with 100 mL of deionized water in order to make a water emulsion in a conical flask (500 mL) and 0.1 g of adsorbent (lignocellulose-clinoptilolite composite) added to the mixture. Each mixture (oil-in-water emulsion + adsorbent) was shaken on an orbital shaker (mrc Orbital shaker) at 160 rpm. Aliquots of the mixture were collected after 5, 15, 30, 60, 180, 300 min. The oil-in-water emulsion was filtered through a 0.45 μm syringe filter after sorption experiments and taken for chemical oxygen demand (COD) measurement. Initial COD and a blank were recorded for each run. All experiments were conducted in duplicate and mean values were used in the analysis of data. COD measurements were done by means of COD Spectroquant Pharo 100 spectrophotometer (Merck) and adsorbed COD was calculated (Equation 1):

$$Q_t = \frac{V(COD_o - COD_e)}{m} \tag{1}$$

where Q is the COD of oil adsorbed (mg g^{-1}) at time, COD$_o$ and COD are the initial and equilibrium CODs (in mg L^{-1}), is the dry mass of adsorbent (g), and is the volume of solution (l).

It is important to note that although ultrasonication was used for the oil-in-water emulsion preparation, aliquots for COD analysis before adsorption could only be collected at specific sites of high emulsion because a surfactant was not used (to obtain a perfect emulsion). COD was considered as the most efficient technique to assess the removal oil because of its complex chemical content (hundreds to thousands of hydrocarbons ranging from C$_{15}$ to C$_{50}$, including a substantial fraction of nitrogen- and sulfur-containing compounds).[49]

3. Results and Discussion

3.1. FT-IR Results

The FT-IR spectra of composites (Fig. 1) and those of the start-ing materials were obtained to study possible changes in the chemical structure of the materials. Peaks were assigned accord-ing to the literature. Except for small shifts (due to the presence of inorganic elements in the structure of clinoptilolite), peaks of composites are the same as those of lignocellulose modified with siloxanes, because silicone is the main element in both the structures of clinoptilolite and siloxanes used for the preparation of the composites.

Therefore, the peak at 805 cm^{-1} was attributed to the symmetri-cal stretching of AlO$_4$ of clinoptilolite or to the Si-C bond present in the siloxane structure.[50] The appearance of peaks between 1150 and 1068 cm^{-1} indicated the presence of a Si–O–Si bridge. But, these peaks may have overlapped with the presence of a C–O bond.[51] The peak at 1269 cm^{-1} was attributed to Si-CH$_3$ bond but also the negligible concentration of C-N (of C-NH$_2$) ending the siloxane. Peaks of small intensity observed at 1319 cm^{-1} and at 1407 cm^{-1} was assigned to the bending mode of –CH$_2$ and –CH$_3$ groups in the molecule. The peak at 1659 cm^{-1} was assigned to the carbonyl group. The peak at 2963 cm^{-1} was due to C-H and 3458 cm^{-1} to O-H. Assignment of peaks was done as reported in the literature.[50–56]

3.2. XRD Analysis

The XRD patterns of the composites (Fig. 2) were obtained to study the effect of lignocellulose and clinoptilolite modified with siloxane on the crystallinity of the composites. Comparison of the untreated grass with the composites shows the difference on the composites patterns. All the composites had their major peaks at around $2\theta \approx 14.5°$, 22.1° and 26.5°, which is quite different from untreated grass. XRD patterns showed changes in the intensity of peaks, likely due to the molecular weight of siloxanes and the scattering of clinoptilolite within the lignocellulosic.

The appearance of the broad peak around 14.5° was attributed to the presence of clinoptilolite in the composites. Also, a minor shift from 21.2° (untreated grass) to 22.1° (composites) was observed and assigned to clinoptilolite.[57,58] In addition, the slightly increased peak intensity observed at 26.6° could have been influenced by clinoptilolite which has a peak in those regions (22° and 26°).[57,58]

3.3. TGA of Lignocellulose-Clinoptilolite Composites

The TGA thermograms of lignocellulose-clinoptilolite com-posites were used to study the thermal stability of composites. Plots (Fig. 3) showed materials having almost the same thermal stability profile. Differences in the slopes were only due to weight loss percentage with the first stage of mass loss around
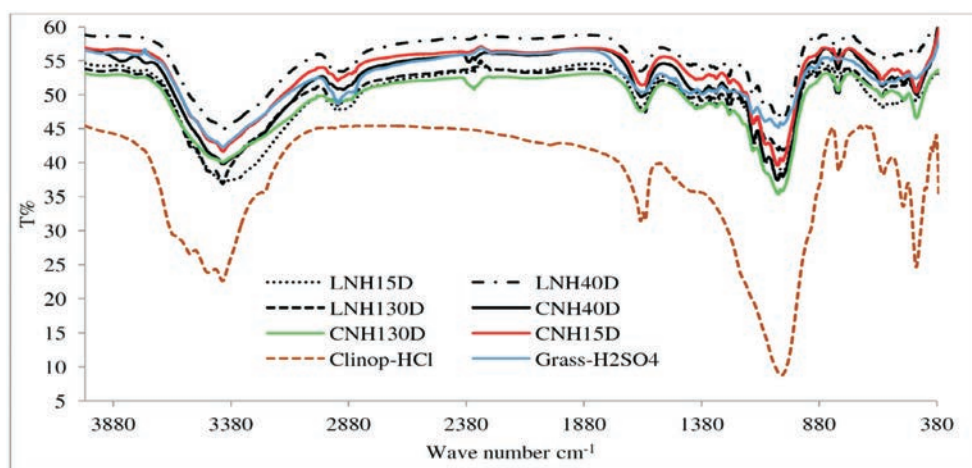

Figure 1 FT-IR of composites and starting materials.

RESEARCH ARTICLE

R.M.K. Vala, L. Tichagwa, H. Pasch and E.D. Dikio,
S. Afr. J. Chem., 2015, **68**, 143–152,
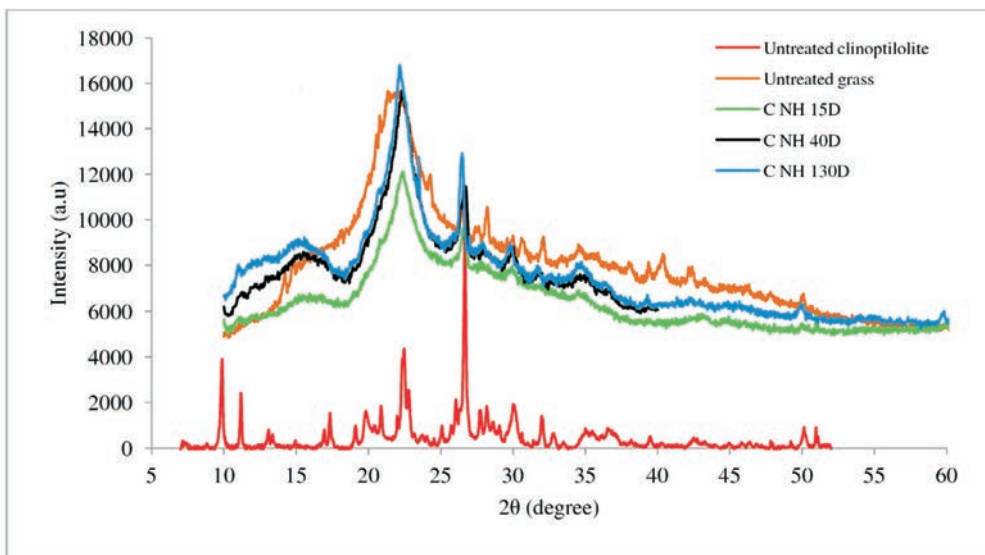<http://journals.sabinet.co.za/sajchem/>.

146

Figure 2 XRD patterns of composites, untreated grass and untreated clinoptilolite.

75–76 °C, ascribed to the water content of the composites.

The second mass loss (around 325 °C for CNH15D, 352 °C for CNH40D and 332 °C for CNH130D) was attributed to the volatile compounds formed during heating. The third but small weight loss (around 459 °C for CNH15D, 484 °C for CNH40D and 489 °C for CNH130D) was probably due to the remaining persistent volatile compounds formed during heat exposure. It was noticed that composite CNH130D has less weight loss (63 %) than CNH15D (74 %) and CNH40D (76 %) suggesting that CNH130D was more thermally stable compared with the other two. The

considerable amount of silicone in the structure of NH130D might have contributed to its high residual weight (NH15D: Mw = 1000 g mol^{-1}; NH40D: Mw = 2600 g mol^{-1}; NH130D: Mw = 11000 g mol^{-1}).

3.4. SEM Analysis

The dispersion of clinoptilolite in the lignocellulosic matrix of the composites was analyzed with SEM. The micrographs (Fig. 4) showed a complete dispersion of clinoptilolite within the lignocellulose matrix to the extent that it could hardly be distin-
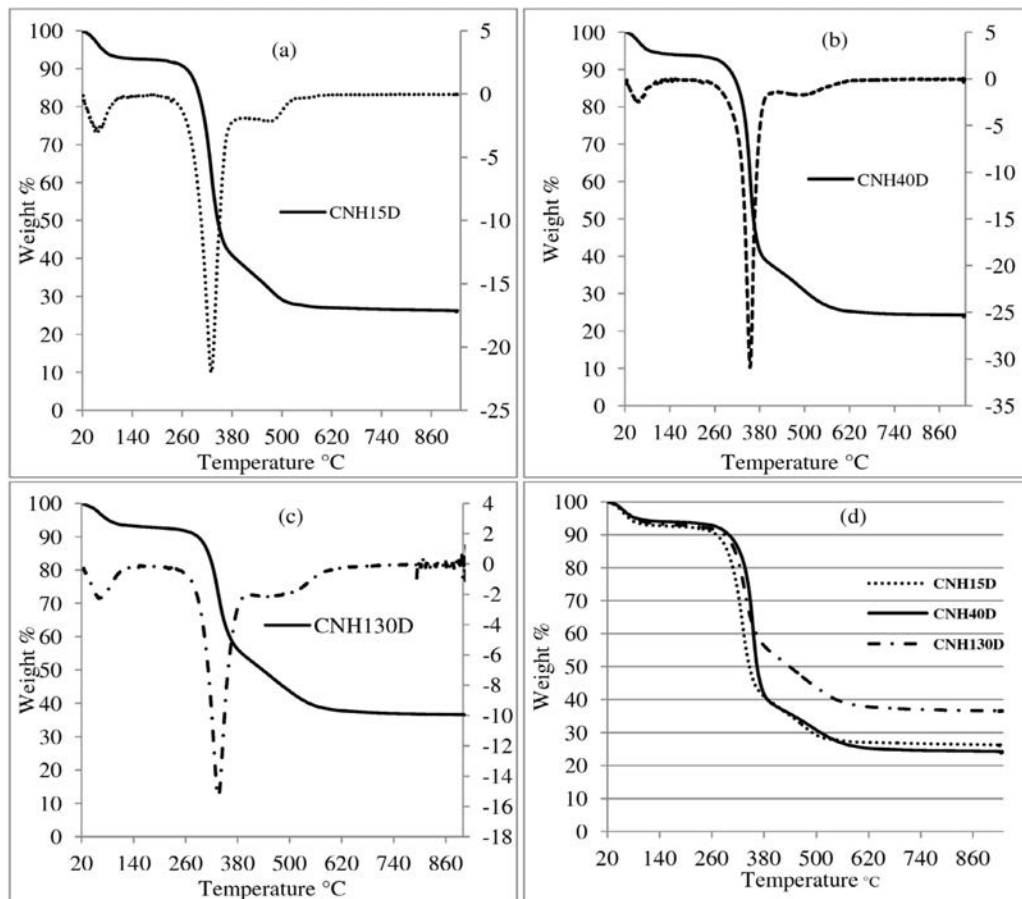

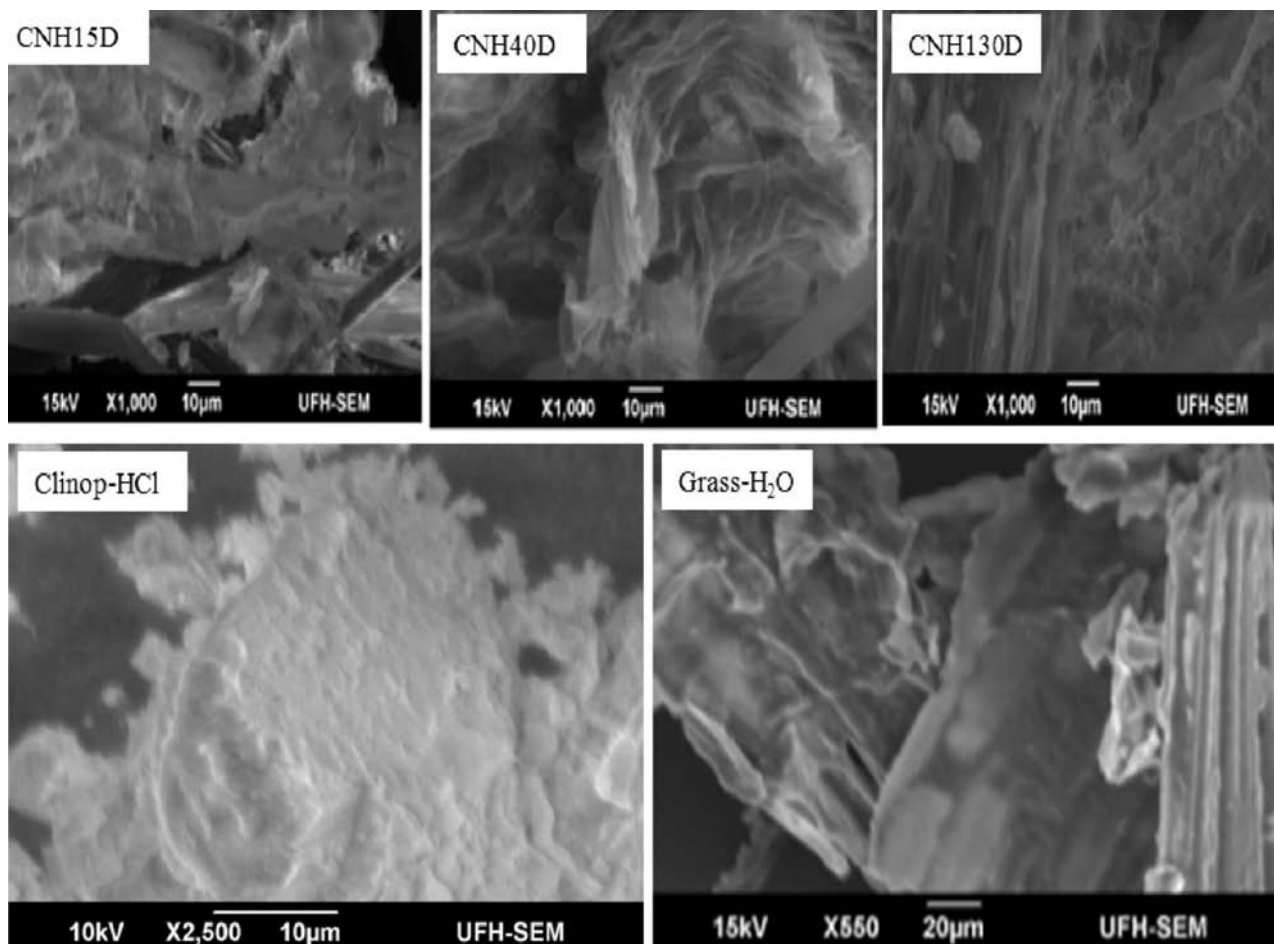**Figure 3** TGA and DTG of composites.

Figure 4 SEM of composites, clinoptilolite and grass.

guished from the other components. This dispersion of clinoptilolite suggested that siloxanes coupling agents played an important role between these two materials to a higher degree.

3.5. Solid State NMR (SS NMR)

Solid State NMR, a suitable technique for the inspection of the structure of hybrid materials,[59] was used to characterize lignocellulose-clinoptilolite composite by means of ^{13}C and ^{29}Si nuclei. The aim of the investigation was to answer the following questions: (1) could the bond between lignocellulose and siloxane be an amide as reported by Gunanathan *et al.*[60] or an ether bond? (2) Can the Si of the repeat unit of the siloxane be distinguished

from 'end-standing' Si bonded to CH_2? (3) Are the Si bonded or associated? (4) Was the composite formed *via* the formation of a chemical bond or *via* association? (5) Can the Si of clinoptilolite (clinop-HCl) be distinguished from those of the siloxane?

3.5.1. ^{13}C Solid State Results

^{13}C NMR spectra (Fig. 5) shows the composite (CNH40D) and the lignocellulose (grass-H_2SO_4). By comparing the CPMAS with CPMAS TOSS spectra, the isotropic signals can be distinguished from spinning sidebands. Almost all signals that appeared in CPMAS also appeared in CPMAS TOSS spectra. Only the peak around 115 ppm could be identified as a spinning sideband.
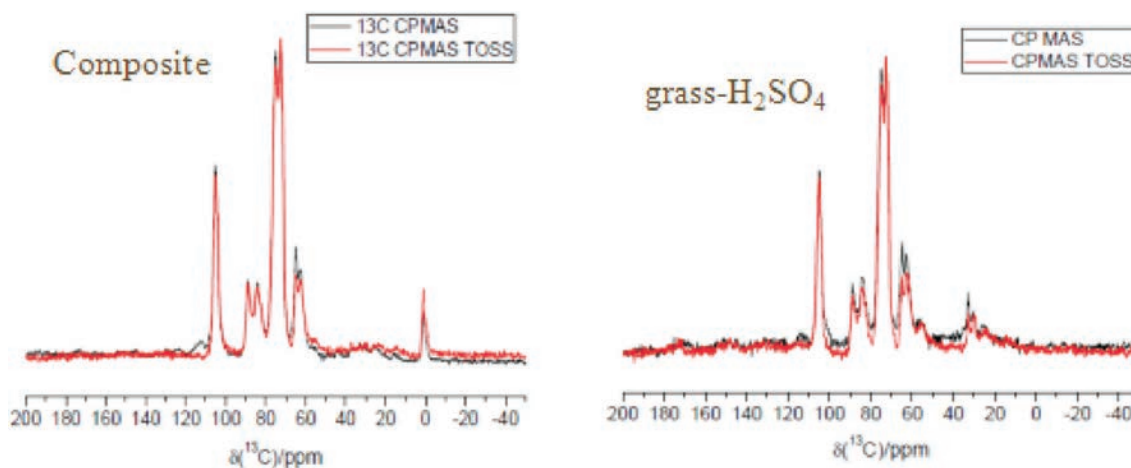

Figure 5 Comparison of $^{13}C\{1H\}$ CPMAS with CPMAS TOSS spectra of the composite (left) and grass-H_2SO_4 (right).

RESEARCH ARTICLE

R.M.K. Vala, L. Tichagwa, H. Pasch and E.D. Dikio,
S. Afr. J. Chem., 2015, **68**, 143–152,
<http://journals.sabinet.co.za/sajchem/>.

148

The CPMAS spectra (Fig. 6) of the composite and grass-H_2SO_4 were compared; using the spectrum of grass-H_2SO_4 as a finger-print spectrum, the lignocellulose components can be clearly identified in the composite. The spectra are very similar, but some differences can be observed: the spectrum of the composite shows an additional signal at 0 ppm (1), which can be assigned to the methyl groups bonded to Si of the repeat unit of the siloxane in the composite. Signal (2) could possibly be a methylene signal of the coupling agent. As reported by Bardet[61], the signal (4) at 62 ppm could be assigned to C of lignin and signal (3) to methoxy groups of lignin. The intensities of these signals were reduced in the composite compared to grass-H_2SO_4 indicating a structural change on the closest carbon of the composite.

It was noted that the signals (5) appearing at 32 ppm were not observed in the spectrum of the composite. An assignment of this signal, however, was not possible as it could not be found in the literature dealing with SS NMR studies on lignocellulose. If signal (5) could be assigned to a component of lignocellulose and was not an impurity, its disappearance in the composite would suggest the formation of a chemically bonded composite rather than a composite formed by association of the components. The cellulose backbone structure was not largely affected by the formation of the composite as indicated by the very similar peak ratio of signal (6) representing crystalline (89 ppm) and amorphous C-4 (84 ppm) signals of cellulose.[62–63]

3.5.2. ^{29}Si SS NMR Results

^{29}Si SS NMR results (Fig. 7) shows the ^{29}Si one-pulse MAS spectra of clinop-HCl measured with and without spinning sideband suppression. By comparison of the spectra of these different methods, the weak signals in the one-pulse MAS spectrum could be identified as spinning sidebands. When ^{29}Si SS NMR spectra of composite and clinop-HCl are compared, four different Si positions in clinop-HCl can be distinguished; they are labelled (1) to (4) (Fig. 8). Assignment of the position of the ^{29}Si in one-pulse MASNMR spectrum (Table 2) was reported by Rivera.[64]

All positions were in the typical chemical shift range of Q^4 units. That means the observed Si atom was bonded to four bridging oxygens and was consequently part of a three-dimensional framework. The notation '(xAl)' referred to the number of Al atoms in the second coordination sphere. For example 'Q^4(2Al)' indicated that the Si atom has two Al atoms and two Si atoms in its second coordination sphere bonded *via* bridging oxygen, respectively. Most of the clinop-HCl signals could be identified in the one-pulse MAS spectrum of the composite, too. Signal (4) could not be observed in the composite; however, this shoulder peak was too weak to be significant and could have been covered under the noise of the spectrum. As indicated (Table 3),

Table 2 Assignment of the position of the ^{29}Si in one-pulse MASNMR spectrum of clinop-HCl.

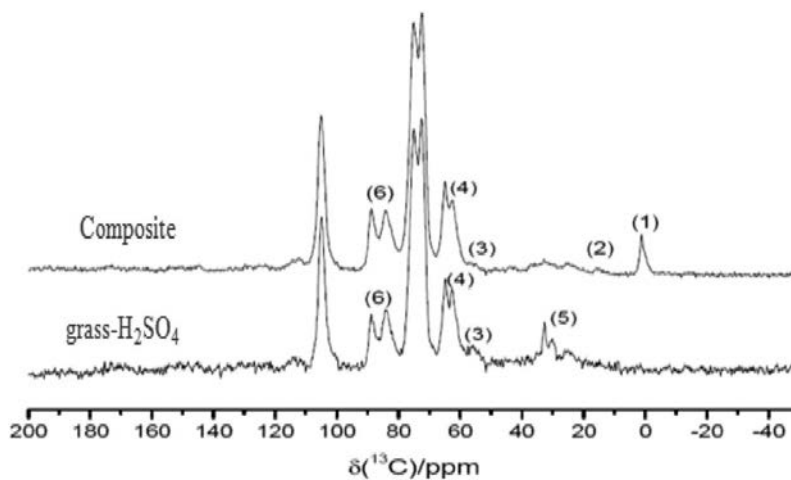| Position	Chemical shift	Assignment[64]
(1)	–112 ppm	Q^4(0Al)
(2)	–107 ppm	Q^4(1Al)
(3)	–100 ppm	Q^4(1Al)
(4)	–91 ppm	Q^4(2Al)

Figure 6 ^{13}C{1H} CPMAS spectra of CNH40D and grass-H_2SO_4.

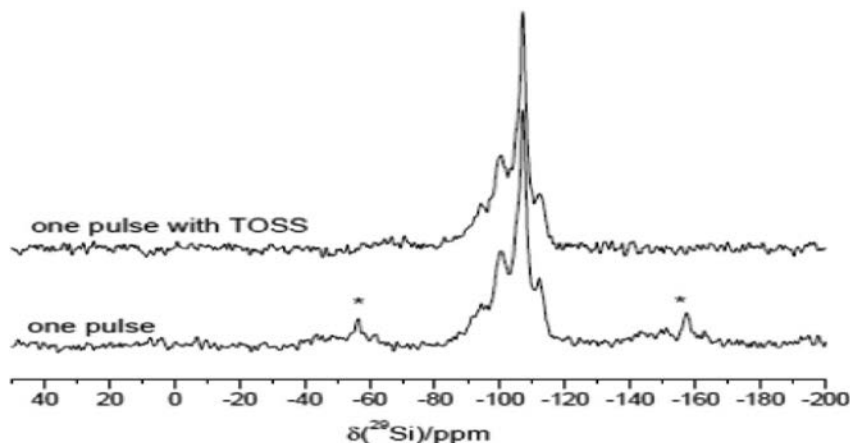**Figure 7** ^{29}Si one-pulse MAS spectra of clinop-HCl with (top) and without TOSS (bottom) (spinning sidebands are marked by an asterisk).
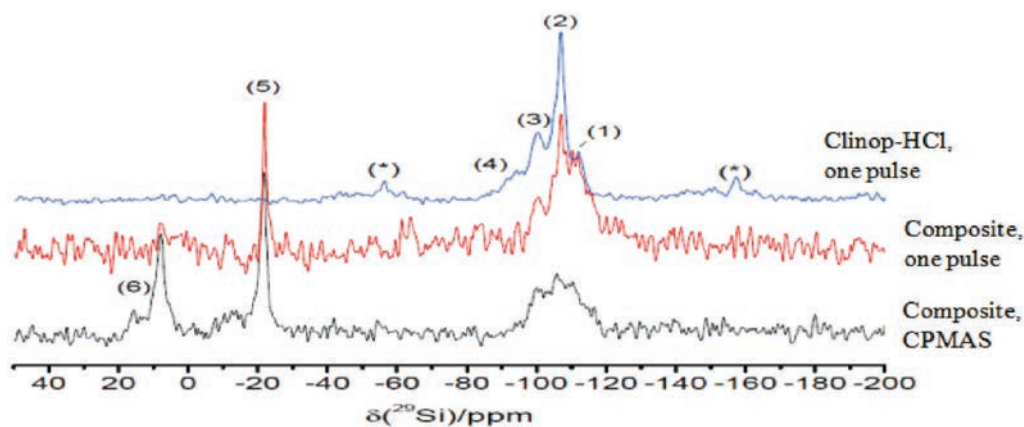
Figure 8 Comparison of ^{29}Si SS NMR spectra of clinop-HCl with the composite (the composite sample was measured using the method's one-pulse MAS and CPMAS).

Table 3 Intensity ratios of the clinoptilolite position 1 and 3 relative to the most intense position 2 in clinop-HCl and the composite.

Ratios	Clinop-HCl (one-pulse MAS)	Composite (one-pulse MAS)
Int (1): Int (2)	0.3	0.8
Int (3): Int (2)	0.4	0.6

the intensity of signal (2) was notably reduced in the composite, implying that the Si atoms present as Q^4(1Al) were affected by the formation of the composite.

The ^{29}Si one-pulse MAS spectrum displayed a clear signal (5) at –22 ppm, which could be assigned to Si of the repeat unit of the coupling agent, which was bonded to two methyl groups. Using the CPMAS technique, an additional peak (6) could be observed. Since its intensity was very large in the CPMAS compared to the one-pulse MAS, a close proximity to protons could thus be deduced. Therefore this signal could be assigned to the end-standing Si atoms in the coupling agent bonded to two methyl groups and one methylene group.

3.6. Adsorption of Used Motor Oil

3.6.1. *Kinetic of Adsorption*

An assessment of the effect of contact time and molecular weight of siloxanes on the adsorption of oil onto composites was conducted, and plots (Fig. 9) revealed that 10 min was enough to adsorb the maximum amount of COD during the process. CNH40D showed slightly higher adsorption properties at the beginning of the process than the other composites whereas, CNH130D (highest siloxane molecular weight) slightly desorbed the oil before they all reach equilibrium. This probably means that the molecular weight of siloxane moiety did not play a visible role during adsorption since the equilibrium is reached almost at the same time (180 min) and with the same amount of adsorbate.

Data (Fig. 10) illustrated good compliance with the pseudo-second-order adsorption with correlation coefficients (R^2) values above 0.999, implying possible chemical interactions between adsorbate and adsorbent.[63] The pseudo-first-order model, however, could not be applied in this case because of their very low correlation coefficients (some $R^2 < 0.1$).
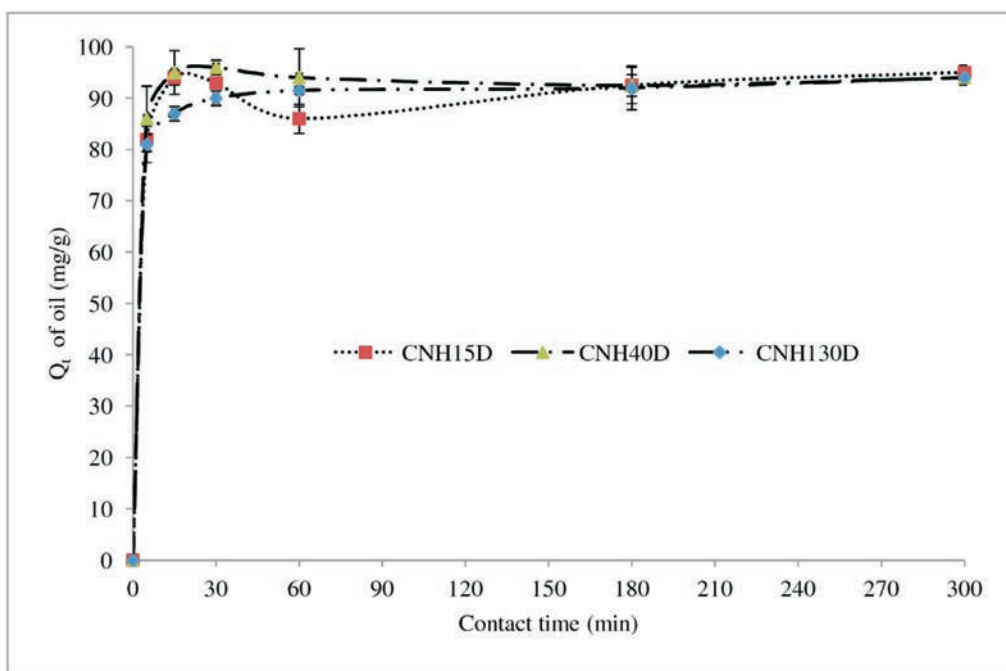

Figure 9 Effect of contact time and siloxanes molecular weight on the removal of oil by composites ($n = 2$).
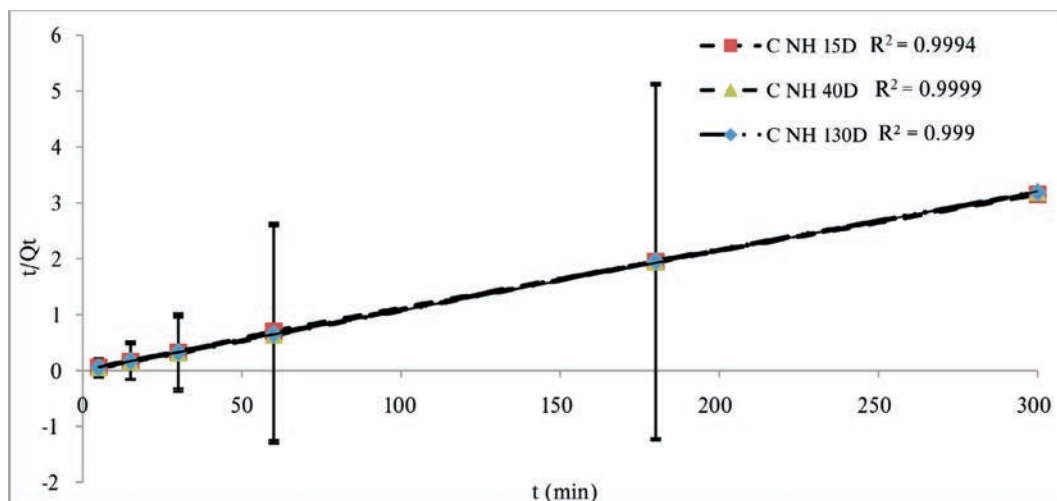
Figure 10 Pseudo-second-order of adsorption of oil onto composites (CNH15D, CNH40D and CNH130D) ($n = 2$).

3.6.2. *Isotherms of Adsorption*

Isotherms (Figs 11 and 12) of oil adsorbed onto the composites showed good R^2 values which permitted to suggest Langmuir model as the best fitting model when compared to the Freundlich model. The R^2 values of the Freundlich model, however, were not too low to be neglected, except for CNH130D ($R^2 = 0.4558$). Therefore, based on isotherms, it is possible to assume that the surface of the adsorbent could be more complex than the monolayer structure suggested by the Langmuir

model,[65–67] because of the complex nature of adsorbents (lignocellulose-siloxane-clinoptilolite).

4. Conclusion

In this study, we prepared lignocellulose-clinoptilolite composites by using N-terminated siloxanes as a coupling agent between the two starting materials: grass-H_2SO_4 and clinop-HCl. ^{13}C and ^{29}Si solid state NMR were used to explore the composite by comparing their spectra to those of the starting materials. It
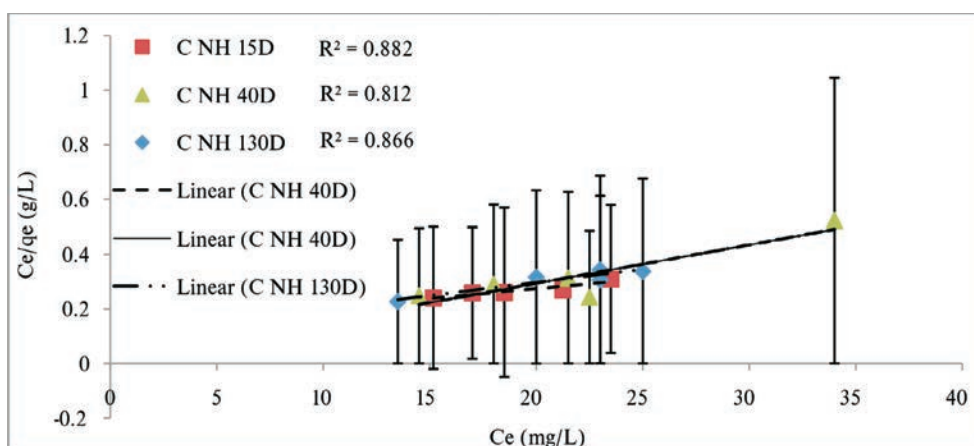

Figure 11 Langmuir isotherms of oil adsorbed onto composites (CNH15D, CNH40D and CNH130D) ($n = 2$).
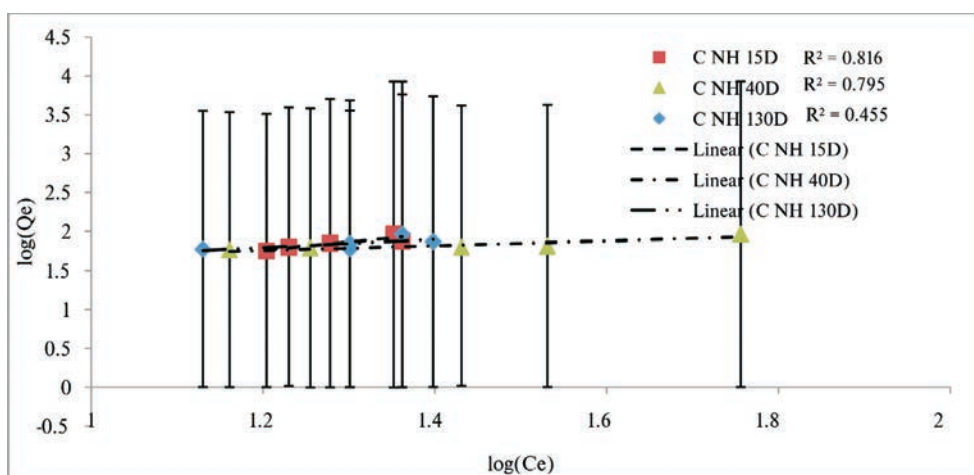

Figure 12 Freundlich isotherms of oil adsorbed onto composites (CNH15D, CNH40D and CNH130D) ($n = 2$).

RESEARCH ARTICLE

R.M.K. Vala, L. Tichagwa, H. Pasch and E.D. Dikio,
S. Afr. J. Chem., 2015, **68**, 143–152,
<http://journals.sabinet.co.za/sajchem/>.

151

was possible to distinguish the carbon signals associated with grass-H_2SO_4 and the composite, and ^{29}Si signals associated with clinop-HCl and the composite. Other techniques (FT-IR, XRD, SEM, and TGA) were also used to explore the properties of the prepared composites. Furthermore, the prepared composites showed good adsorption properties by removing 92 mg g^{-1} of COD of oil.

Acknowledgement

References

1 S.J. Eichhorn, C.A. Baillie, N. Zafeiropoulos, L.Y. Mwaikambo, M.P. Ansell, A. Dufresne, K.M. Entwistle, P.J. Herrera-Franco, G.C. Escamilla, L. Groom, M. Hughes, C. Hill, T.G. Rials and P.M. Wild, Review: Current international research into cellulosic fibres and composites, *J. Mater. Sci.*, 2001, **36**, 2107 – 2131.

2 L Avérous and N. Boquillon, Biocomposites based on plasticised starch: thermal and mechanical behaviours, *Carbohyd. Polym.*, 2004, **56**(2), 111–122.

3 M.J. John, R.D. Anandjiwala, L.A. Pothan and S. Thomas, Cellulosic fibre-reinforced green composites, *Compos. Interface*, 2007, **14**(7-9), 733–751.

4 M.J. John and S. Thomas, Review: Biofibres and biocomposites, *Carbohyd. Polym*, 2008, **71**, 343–364.

5 T. Nishino and N. Arimoto, All-Cellulose Composite Prepared by Selective Dissolving of Fiber Surface, *Biomacromolecules,* 2007, **8**, 2712–2716.

6 C.J. Brinker and G.W. Scherer, *Sol-Gel Science: The Physics and Chemistry of Sol-Gel Processing*, Academic Press, San Diego, California, USA, 1990.

7 J.M. Duval, A.J.B. Kemperman, B. Folkers, M.H.V. Mulder, G. Desgrandchamps and C.A. Smolders, Preparation of zeolite filled glassy polymer membranes, *J. Appl. Polym. Sci.*, 1994, **54**, 409–418.

8 N. Soykeabkaew, N. Arimoto, T. Nishino, T. Peijs, All-cellulose composites by surface selective dissolution of aligned ligno-cellulosic fibres, *Compos. Sci. Technol.*, 2008, **68**, 2201–2207.

9 H.L. Bos, J. Mussig and M.J.A. Van den Oever, Mechanical properties of short-flax-fibre reinforced compounds, *Composites: Part A*, 2006, **37**(10), 1591–1604.

10 A. Gomes, T. Matsuo, K. Goda and J. Ohgi, Development and effect of alkali treatment on tensile properties of curaua fiber green composites, *Compos. Part A-Appl S*, 2007, **38**(8), 1811–1820.

11 X. Li, L.G. Tabil and S.J. Panigrahi, Chemical treatments of natural fiber for use in natural fiber-reinforced composites: a review, *Polym. Environ.*, 2007, **15**(1), 25–33.

12 O.Y. Mansour Lignocellulose–polymer composite III, *J. Appl. Polym. Sci.*, 1993, **47**(5), 839–846.

13 S.M. Serino, A.L. Garofalo, M.N. Goeser and M.J. Deaner, Polymer covered advanced polymer/wood composite structural member, *US Pat.* 6357197 (2002).

14 Z. Lin and S. Renneckar, Nanocomposite-based lignocellulosicfibers 2: Layer-by-layer modification of wood fibers for reinforcement in thermoplastic composites, *Composites: Part A*, 2011, **42**, 84–91.

15 T. Bunhu and L. Tichagwa, Adsorption of methyl orange, Pb^{2+} and Cd^{2+} from aqueous solution by composites of lignocellulose-montmorillonite modified with methacryloxypropyl trimethoxysilane, *Macromol. Symp.*, 2012, **313–314**, 146–156.

16 E.D. Fisher, W. Wypart and Kristofferson Marcus, Wood-polymer-zeolite composites, *US Pat. N US 7,550,404 B2* (2009).

17 L.I. Bel'chinskaya, Strel'nikova O. Yu, L.A. Novikova, F. Ressner and O.V. Voishcheva, Enhancement of the adsorption selectivity of nanoporous clinoptilolite by hydrophobization with organosiloxanes, *Prot Met+*, 2008, **44**(4), 390–393.

18 A. Zampieri, S. Kullmann, T. Selvam, J. Bauer, W. Schwieger, H. Sieber, T. Fey, and P. Greil, Bioinspired rattan-derived SiSiC/Zeolite monoliths: preparation and characterization, *Micropor. Mesopor. Mat.*, 2006, **90**(1-3), 162–174.

19 S. Mintova and V. Valtchev, Preparation of zeolite-covered cellulose fibers, Abstract of Papers, 209th ACS National Meeting, *A.C.S.* (1995).

20 J. Troquet, C. Larroche and C.G. Dussap, Evidence for the occurrence of an oxygen limitation during soil bioremediation by solid-state fermentation, *Biochem. Eng. J.*, 2003, **13**, 103–112.

21 B. Antizar-Ladislao, J. Lopez-Real and A.J. Beck, Laboratory studies of the remediation of polycyclic aromatic hydrocarbon contaminated soil by invessel composting, *Waste Manag.*, 2005, **25**, 281–289.

22 B. Antizar-Ladislao, J. Lopez-Real and A.J. Beck, Degradation of polycyclic aromatic hydrocarbons (PAHs) in an aged coal-tar contaminated soil under in-vessel composting conditions, *Environ. Pollut.*, 2006, **141**, 459–468.

23 R. Vazquez-Duhalt, Environmental impact of used motor oil: review, *Sci. Total Environ.*, 1989, **79**(1), 1–23.

24 E. Clonfero, B. Nardini, M. Marchioro, A. Bordin and G. Gabbani, Mutagenicity and contents of polycyclic aromatic hydrocarbons in used and recycled motor oils, *Mutat. Res-Genet. Tox.*, 1996, **368**(3-4), 283–291.

25 M. Granella, C. Ballarin, B. Nardini, M. Marchioro and E. Clonfero, Mutagenicity and contents of polycyclic aromatic hydrocarbons in new high-viscosity naphthenic oils and used and recycled mineral oils, *Mutat. Res.*, 1995, **343**, 145–150.

26 J.F. Nash, S.D. Gettings, W. Diembeck, M. Chudowski and A.L. Kraus, A toxicological review of topical exposure to white mineral oils, *Fd. Chem. Toxic.*, 1996, **34**(2) 213–225.

27 I.N.E. Onwurah, V.N. Ogugua, N.B. Onyike, A.E. Ochonogor and O.F.Otitoju, Crude oil spills in the environment, effects and some innovative clean-up biotechnologies, *IJER,* 2007, **1**(4), 307–320.

28 H. Lefcort, K.A. Hancock, K.M. Maur and D.C. Rostal, The effects of used motor oil, silt, and the water mold *Saprolegnia parasitica* on the growth and survival of mole salamanders (genus *Ambystoma*), *Arch. Environ. Contam. Toxicol.*, 1997, **32**, 383–388.

29 R.F. Johnson and T.G. Manjrekar, Removal of oil from water surfaces by sorption on unstructured fibers, *Environ. Sci. Technol.*, 1973, **7**, 439–443.

30 Ch. Teas, S. Kalligeros, F. Zanikos, S. Stournas, E. Lois and G. Anastopoulos, Investigation of the effectiveness of absorbent materials in oil spill clean up, *Desalination*, 2001, **140**, 259–264.

31 Q.F. Wei, R.R. Mather, A.F. Fotheringham and R.D. Yang, Evaluation of nonwoven polypropylene oil sorbents in marine oil-spill recovery, *Mar. Pollut. Bull.*, 2003, **46**, 780–783.

32 S.A. Sayed and A.M. Zayed, Investigation of the effectiveness of some adsorbent materials in oil spill clean-ups, *Desalination*, 2006, **194**, 90–100.

33 A. Gammoun, S. Tahiri, A. Albizane, M. Azzi, J. Moros, S. Garrigues and M. de la Guardia, Separation of motor oils, oily wastes and hydrocarbons from contaminated water by sorption on chrome shavings, *J. Hazard. Mater.*, 2007, **145**, 148–153.

34 V. Rajaković-Ognjanović, G. Aleksić and L. Rajaković, Governing factors for motor oil removal from water with different sorption materials, *J. Hazard. Mater.*, 2008, **154**(1-3), 558–563.

35 H. Moriwaki, S. Kitajima, M. Kurashima, A. Hagiwara, K. Haraguchi, K. Shirai, R. Kanekatsu and K. Kiguchi, Utilization of silkworm cocoon waste as a sorbent for the removal of oil from water, *J. Hazard. Mater.*, 2009, **165**, 266–270.

36 R.M. Barrer and M.B. Makki, Molecular sieve sorbents from clinoptilolite, *Can. J. Chem.*,1964, **2**, 1481–1487.

37 M.P. Elizalde-González, J. Mattusch, R. Wennrich and P. Morgenstern, Uptake of arsenite and arsenate by clinoptilolite-rich tuffs, *Micropor. Mesopor. Mat.*, 2001, **46**(2-3), 277–286.

38 A. Top and S. Ülkü, Silver, zinc, and copper exchange in a Na-clinoptilolite and resulting effect on antibacterial activity, *Appl. Clay Sci.* 2004, **27**(1-2), 13–19.

39 H. Faghihian and M. Pirouzi, Cis/trans-but-2-ene adsorption on natural and modified clinoptilolite, *Clay Minerals*,2009, **44**, 405–409.

40 R. Ruiz and T. Ehrman, Dilute acid hydrolysis procedure for determination of total sugars in the liquid fraction of process samples, in *Chemical Analysis and Testing Task Laboratory Analytical Procedure*, LAP-014, Department of Energy, Washington, 1996.

41 L. Palmowski and J. Muller, Influence of the size reduction of organic waste on their anaerobic digestion, in *II International Symposium on Anaerobic Digestion of Solid Waste,* Barcelona, 1999, **15–17**, 137–144.

42 H. Shibazaki, S. Kuga, F. Onabe and R.M. Brown Jr, Acid hydrolysis behaviour of microbial cellulose II, *Polymer*, 1995, **36**(26), 4971–4916.

43 N. Curreli, M. Agelli, B. Pisu, A. Rescigno, E. Sanjust and A. Rinaldi, Complete and efficient enzymatic hydrolysis of pretreated wheat straw, *Process. Biochem.*, 2002, **37**, 937–941.

44 Q. Xiang, Y.Y. Lee, P.O. Pettersson and R.W. Torget, Heterogeneous aspects of acid hydrolysis of α-cellulose', *Appl. Biochem. Biotech.*, 2003, **107**(1-3), 505–514.

45 F. Hong and K. Qiu, An alternative carbon source from konjac powder for enhancing production of bacterial cellulose in static cultures by a model strain *Acetobacter aceti* subsp. *xylinus* ATCC 23770, *Carbohyd. Polym*, 2008, **72**, 545–549.

46 M.C. Matías, M.U. De La Orden, C. González Sánchez and J. Martínez Urreaga, Comparative spectroscopic study of the modification of cellulosic materials with different coupling agents, *J. Appl. Polym. Sci.*, 2000, **75**, 256–266.

47 F. Le Digabel, N. Boquillon, P. Dole, B. Monties and L. Averous, Properties of thermoplastic composites based on wheat-straw lignocellulosic fillers, *J. Appl. Polym. Sci.*, 2004, **93**(1), 428–436.

48 F. Cao, P. Bai, H. Li, Y. Ma, X. Deng and C. Zhao, Preparation of polyethersulfone-organophilic montmorillonite hybrid particles for the removal of bisphenol A, *J. Hazard. Mater.*, 2009, **162**, 791–798.

49 ABB-Environmental, Compilation of data on the composition, physical characteristics and water solubility of fuel products, Prepared for Massachusetts Department of Environmental Protection, Wakefield, Massachusetts, 1990.

50 H. Faghihian, M. Talebi and M. Pirouzi, Adsorption of nitrogen from natural gas by clinoptilolite, *J. Iran. Chem. Soc.*, 2008, **5**(3), 394–399.

51 J. Coates, Interpretation of infrared spectra: a practical approach, in *Encyclopaedia of Analytical Chemistry*, (R.A. Meyers, ed.), John Wiley & Sons, New York, NY, USA, 2000, pp. 10815–10837.

52 D.W. Brown, A.J. Floyd and M. Sainsbury, *Organic Spectroscopy*, John Willey & Sons, New York, NY, USA, 1988.

53 W. Kemp, *Organic spectroscopy*, 3rd edn, ELBBS & McMillan, City, UK, 1991.

54 H. Homma, T. Kuroyagi, K. Izumi, C.L. Mirley, J. Ronzello and S.A. Boggs, Diffusion of low molecular weight siloxane from bulk to surface, *IEEET Dielect El In*, 1999, **6**(3), 370–375.

55 E. Hamciuc, C. Hamciuc and M. Cazacu, Poly(1,3,4-oxadiazole-ether-imide)s) and their polydimethylsiloxane-containing copolymers, *Eur. Polym. J.*, 2007, **43**, 4739–4749.

56 B. Mohebby and R.Hadjihassani, Moisture repellent effect of acetylation on poplar fibres, *J. Agric. Sci. Technol.*, 2008, **10**, 157–163.

57 G.M. Arifuzzaman Khan, S.M.Y. Arafat, M.N. Reza, S.M. Abdur Razzaque & Md. Shamsul Alam, Linde Type-A zeolite synthesis and effect of crystallization on its surface acidity, *Indian J. Chem. Technol.*, 2010, **17**, 303–308.

58 A.A. Kittur,M.Y. Kariduraganavar, U.S. Toti, K. Ramesh,T.M. Aminabhavi, Pervaporation Separation of Water–Isopropanol Mixtures Using ZSM-5 Zeolite Incorporated Poly(vinyl alcohol) Membranes, *J. Appl. Polym. Sci.*, 2003, **90**(9), 2441–2448.

59 T. Takayama, Inorganic polymers, in *Solid State NMR of Polymers*, (I. Ando and T. Asakura, eds.), Elsevier, Amsterdam, 1998.

60 C. Gunanathan, Y. Ben-David and D. Milstein, Direct synthesis of amides from alcohols and amines with liberation of H_2, *Science*, 2007, **317**(5839), 790–792.

61 M. Bardet, M.F. Foray and Q.K. Trân, High-resolution solid-state CPMAS NMR study of archaeological woods, *Anal. Chem.*, 2002, **74**, 4386–5390.

62 T. Liitiä, S.L. Maunu and B. Hortling, Solid state NMR studies on cellulose crystallinity in fines and bulk fibres separated from refined kraft pulp, *Holzforschung*, 2000, **54**, 618–624.

63 R.H. Newman and J.A. Hemmingson, Determination of the degree of cellulose crystallinity in wood by carbon-13 nuclear magnetic resonance spectroscopy, *Holzforschung*, 1990, 44, 351–355.

64 A. Rivera, T. Farías, A.R. Ruiz-Salvador and L.C. de Ménorval, Preliminary characterization of drug support systems based on natural clinoptilolite, *Micropor. Mesopor. Mat.*, 2003, 61, 249–259.

65 Y.S. Ho and G. McKay, Pseudo-second order model for sorption processes, *Process Biochem.*, 1999, **34**, 451–465.

66 M.D. Levant and T. Vermeulen, Binary Langmuir and Freundlich isotherms for ideal adsorbed solutions, *J. Phys. Chem.*, 1981, **85**, 3247–3250.

67 K.S.W. Sing, D.H. Everett, R.A.W. Haul, L. Moscou, R.A. Pierotti, J. Rouquerol and T. Siemiewska, Reporting physisorption data for Gas/solid systems with special reference to the determination of surface area and porosity, *Pure App. Chem.*, 1985, **57**(4), 603–619.